Tellus (1992), *44B*, 469–488

Meteorological characteristics of the Po Valley fog

By W. WOBROCK, D. SCHELL, R. MASER, M. KESSEL, W. JAESCHKE, *Zentrum für Umweltforschung, Johann Wolfgang Goethe-Universität, Robert-Mayer-Str. 7–9, D-6000 Frankfurt a.M., Germany*, S. FUZZI, M. C. FACCHINI, G. ORSI, *Istituto FISBAT-CNR, Via de Castagnoli 1, 40126 Bologna, Italy*, A. MARZORATI, *ENEL/DSR/CRTN, Via Rubattino 54, 20134 Milano, Italy*, P. WINKLER, *Deutscher Wetterdienst, Meteorologisches Observatorium Hamburg, Frahmredder 95, D-2000 Hamburg, Germany*, B. G. ARENDS, *Netherland Energy Research Foundation, P.O. Box 1, 1755 ZG Petten, The Netherlands*, J. BENDIX, *Geographisches Institut, Universität Bonn, Meckenheimer Allee 166, D-5300 Bonn, Germany*

(Manuscript received 29 November 1991; in final form 11 June 1992)

ABSTRACT

The meteorological situation during the first joint field campaign from 10–17 November 1989 of the EUROTRAC subproject GCE is discussed. The synoptic situation is illustrated by weather charts and satellite pictures. Backtrajectories were calculated in order to identify the origins of airmasses reaching the observation point. Model calculations were performed to explain the observed counter current channelling in the Po Valley. For the 5 different fog episodes observed, fog liquid water content, temperature, humidity, and wind speed are displayed as a function of height. Possible reasons for formation, evolution, and dissipation are discussed. It was found that the radiation effects only played a minor role. Most of the time, the fog at the observation site was either advected or formed due to the advection of cold or moist air.

1. Introduction

A number of fog field campaigns have been performed over the last two decades. Among those were the radiation fog experiments in the UK (at Cardington, 1971–73) by Roach et al. (1976), in Germany (at Meppen, 1978) by Choularton et al. (1981), and in the USA (at Albany, NY, 1982 and 1985) by Jiusto and Lala (1983) resp. Fitzjarrald and Lala (1989) as well as the valley fog experiment (at Elmira, NY, 1970) by Pilié et al. (1975).

The general objective of these experiments was the understanding of dynamic and thermodynamic processes leading to fog formation, evolution, and dissipation in order to advance in fog prediction.

The Meppen fog experiment (1978) and the valley fog experiment (at Elmira, 1970) also put special emphasis on the microphysics of fog. The Albany fog experiments, in addition, extensively investigated the role of surface and boundary layer fluxes in order to determine fog onset time and ultimate fog thickness as well as the deposition of fog droplets onto different surfaces (Wattle et al., 1984).

In contrast to these fog field campaigns, the main objective of the Po Valley experiment, carried out 10–17 November 1989 by the EUROTRAC subproject GCE (ground based cloud experiment), was mainly devoted to improving our understanding of the physico-chemical properties in ground fogs with respect to gas phase and liquid water chemistry and cloud and aerosol microphysics. Thus, the general aim of the Po Valley experiment was clearly different from those mentioned above. Nevertheless, this campaign also required a detailed description of the meteorological situation leading to the long lasting fog periods, and explanation of the mesoscale environment responsible for the wind field in the Po Valley, and an extensive investigation of the micrometeorological evolution for all fog events, 10–17 November 1989. This will be attempted in the present paper, thus, providing the background for the associated papers on fog microphysics and chemistry in this issue.

After a short description of the measurement site and the experimental set-up, Section 3 will display the time evolution of the large scale situation supported by high resolution NOAA-AHVRR satellite pictures, and some investigations on the observed wind in the valley are presented. Finally, most relevant meteorological parameters for each fog event are illustrated and discussed in Section 4. In this context also a physical explanation for the fog formation, evolution and dissipation processes will be attempted.

2. Measuring site and experimental set-up

The observation point was located at the meteorological base San Pietro Capofiume (44.66° N, 11.61° E, 10 m elevation) about 40 km north east of Bologna (Italy) very close to the center of the Po Valley (see Fig. 1 in Fuzzi et al., 1992).

The valley of the river Po extends in west-east direction over 350 km and is 100–150 km wide. It is surrounded in the north and west by the steep mountains of the Alps and in the south by the Apennines which also quickly gain heights above 2000 m.

The field site was located about 30 km south of the river Po and about 1.5 km southwest of the river Reno in a very flat and almost horizontally homogeneous terrain of grassland and harvested fields. The only inhomogenities were created by a few farm houses, isolated standing trees, and bushes. The measurement site itself included next to the equipment of the GCE campaign an aerological station.

The complete experimental equipment of the field campaign is described in Fuzzi et al. (1992). From the large number of measurements made only the following were used for the evaluation presented in this paper: temperature, wind speed and direction, relative humidity and shortwave radiation from the tower and the ground level. Additionally in the ground level longwave radiation fluxes were observed for the determination of the surface temperature.

For the observation of the horizontal and vertical wind up to 660 m we used the data of the 3D Doppler Sodar System.

During the period from 13–17 November 1989 additional radiosoundings were performed measuring dry and wet bulb temperature as well as pressure (AIR, Inc. Airsonde) up to 3000 m in 25 m intervals.

From the number of liquid water observations taken during the campaign this paper only considers the results from the optical probes FSSP-100 and the liquid water indicator PVM100 (Gerber, 1987). One FSSP-100 and the PVM100 were operated at 1.5 m, the second FSSP-100 was attached to the tower elevator. The elevator ascended the tower (51 m) every hour on the hour and descended again. This took about 10–15 min. The rest of the hour the elevator platform was standing in 25 m.

The time resolution for most measurements was one minute except for the radiation measurements, which took place at 2-min intervals.

The Doppler Sodar observations were averages over 10 min in the period from 11–15 November 1989 and 30-min averages for the other days. The radiosondes for temperature and humidity were launched every 3 h (starting from 13 November) except at 11:00 and 23:00 local time where the routine aerological measurements of the meteorological base at San Pietro were used.

Unfortunately, some of the above mentioned measurements are not available continuously over the entire campaign as power and computer failures and other technical problems occurred for minutes up to hours.

3. Meteorological analysis for the period 10–17 November 1989

3.1. *Synoptic description*

The general weather situation for the period from 10–17 November 1989 was determined by the development of a high pressure ridge and its intensification to a blocking high over Middle Europe.

Prior to this evolution Northern Italy was crossed by the southern branch of an aged and occluded front, which was bringing showers in the afternoon of 9 November at the measurement site. During the following night the low pressure system with its center over the North Sea drifted eastward and its southern branch reaching from East Europe down to the Mediterranean Sea disappeared completely. The distance to the next

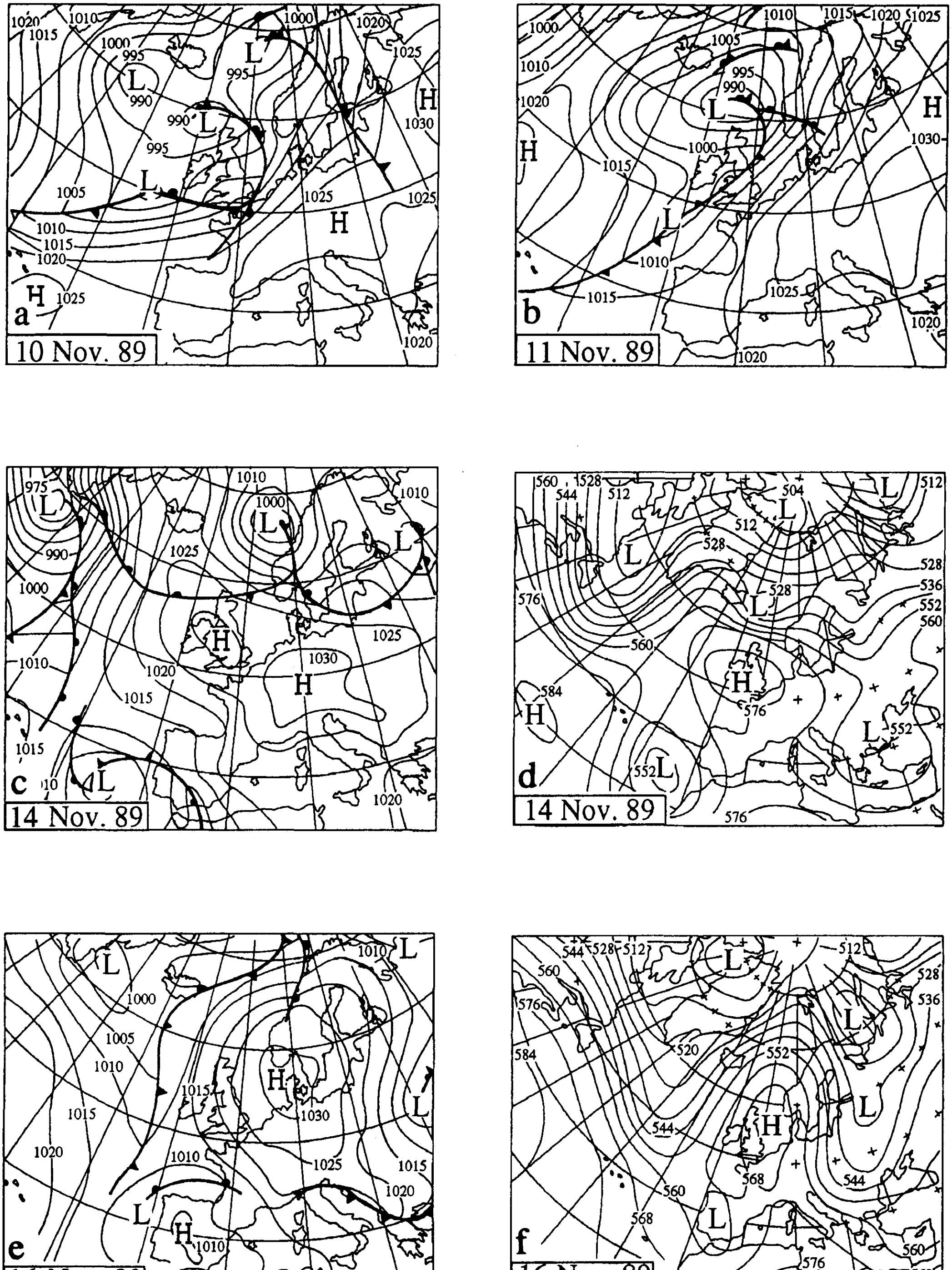

Fig. 1. Weather charts for surface (06:00 UTC) and 500 hPa (00:00 UTC).

cyclonic system moving in from the North Atlantic (Fig. 1a) was large enough so that a high pressure ridge could build up reaching from the Mediterranean Sea to Middle Europe. This high-pressure wedge developed within the next 24 h into a huge continental anticyclone with its center over East Europe (Fig. 1b).

During the 3 following days, the system intensified (Fig. 1c) and a closed high pressure circulation also built up in the upper troposphere (Fig. 1d). As the system aloft developed detached from the one at the surface it is called a "cutoff high". Such cutoff highs which are well-known in the synoptic literature (Petterssen, 1956) are often coupled to cutoff lows to the Southwest and the Southeast and thereby form an Ω shaped pattern (Fig. 1d, f). A further consequence of the blocking high was that incoming cyclonic disturbances were deviated towards the north whereby a chain of cyclones formed, reaching from the North Atlantic along Scandinavia up to Northeast Europe (Fig. 1c). Hence, this blocking high caused stable fair weather conditions for the following five days in North Italy which even lasted until 21 November in Middle and Central East Europe.

Due to the strong radiative cooling under cloud free conditions, a ground inversion formed up to 450 m during the night of 10, 11 November in the Po Valley. This inversion persisted until noontime of 15 November when the subsidence of warm and dry air from the high pressure system into the boundary layer became effective.

On 16 November, the continental anticyclone had migrated to Northeast Europe and the cyclonic flow of the southeastern edge of the Ω pattern had enhanced significantly. Consequently, a new cold front along the Adriatic Sea down to Greece formed (Fig. 1e), and influenced strongly the weather conditions at the measurement site. During daytime of 16 November North Italy was covered partly by clouds and in the morning of 17 November deep cloud cover was present.

In the course of 17 November this southeastern cold front linked to the warm front of a low over the South of Spain. This new frontal system determined the weather in North Italy for the next days as it went along with heavy rain showers.

3.2. *Airmasses in the free atmosphere*

From the series of weather charts illustrated in Fig. 1 it is obvious that the airmasses flowing into North Italy between 10 and 17 November came from various different origins. In Fig. 2, the trajectories in the 850 hPa level for each day are displayed. They were calculated by means of the iterative isobar model of the Mainz University basing on the method described in Pettersson (1956). Each trajectory gives the course of the airmass for the preceding three days in intervals of 12 h (indicated by the •). Next to every trajectory date and time of arrival at the measurement site are listed.

Fig. 2a and b show that a distinct change in airmass happened during 12 November, 12:00 and 13 November, 00:00. Prior to this, the airmasses came from the west and turned into the Po Valley over north and northeast. From 13 November on, the air-masses came from eastern and northeastern directions.

This change between 12 and 13 November was caused by the development of the high in the upper levels. As can been seen from the 500 hPa charts (see Fig. 1) and has already been discussed above,

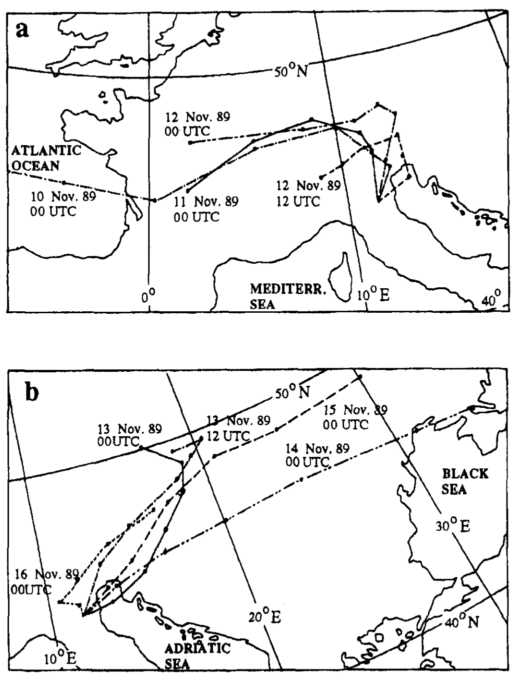

Fig. 2. Backtrajectories for the air masses in 850 hPa for the period from 10–16 November 1989. The trajectories are calculated for the preceding three days in steps of 12 h.

the meandering zonal current had split so that the main current swung around the anticyclone while a secondary current penetrated along the base of the Ω shaped pattern. This secondary current was responsible from 13 November on for the flow of air mass coming from northeast, i.e., from East Europe. This situation persisted until the end of the campaign.

These differences in airmass were also registered by the chemical measurements in the surface layer. On 12 November, the concentration of HNO_3 and the pollutants in the fog water (Facchini et al., 1992) were significantly higher than afterwards as during this time the air-masses were coming for the last 72 h from the western part of the Po Valley itself while on 13 November the airmasses originated from a much greater distance far away in East Europe. This change in the large-scale flow was not visible in the wind direction in the surface levels due to a channelling effect of the Po Valley.

3.3. *Airflow in the surface level*

The trajectory analysis for 850 hPa (Fig. 2) as well as the isobar-figures for the 500 hPa level (Fig. 1) indicate that the wind in the higher levels mostly came from northeastern directions down across the Po Valley. The only exception from the north eastern direction was reported on 15 and 16 November, most likely due to the influence of the low over Southeast Europe as already described in Subsection 3.1). In Table 1, the observations for wind direction and speed at 23:00 and 11:00 local time for 850 hPa at San Pietro are summarized. In Fig. 3a and b the corresponding wind direction in the surface level for 10 and 50 m are illustrated. Surprisingly, the surface winds flowed for most of the time in western and northwestern directions with the exception of the above mentioned days.

The phenomenon that an air flow crossing a valley under any angle is deviated into a direction which is almost that of the valley is called channelling. Furthermore, we notice here that for our directions of the geostrophic wind (i.e., the wind in 850 hPa) the surface wind in the Po Valley had almost the opposite direction (especially the wind component parallel to the valley). This is a so-called counter current.

A theoretical explanation for this phenomenon was given, e.g., by Wippermann (1984). Wippermann applied an analytical model to the upper Rhine valley (north–south direction, 300 m depth and 35 km broad) where both phenomena are often observed and found reasonable agreement between observation and model. His analytical model considers a straight valley with homogeneous conditions along the center line, thus derivatives along the valley vanish. Further model assumptions are: stationarity, neutral stratification, barotropy, the air flow follows the terrain, no advection and a simple parametrization for the vertical friction F_z in the following form

$$F_z = \lambda \boldsymbol{v} - \mu(\boldsymbol{k} \times \boldsymbol{v}).$$

$\boldsymbol{v}$ is the wind vector, $\boldsymbol{k}$ the vertical unit vector, the coefficients for the friction λ and μ are given in Wippermann (1984).

We have applied this analytical model to our situation with a valley in west-east direction (100 km broad, 500 m deep see Fig. 4a). Thus, the resulting equations for the zonal and meridional components u and v of the horizontal wind are:

$$-f(v - v_g) = \mu v - \lambda u,$$

$$f(u - u_g) = -\lambda v - \mu u \frac{1}{\rho_0} \frac{\partial p^*}{\partial x},$$

$$\frac{\partial}{\partial y} \rho_0 (H - h) = 0.$$

Table 1. *Wind direction and wind speed (ms^{-1}) at 850 hPa for 11 and 23 UTC observed at the aerological station San Pietro Capofiume, 10–17 November 1989*

November	10		11		12		13		14		15		16		17
time	11	23	11	23	11	23	11	23	11	23	11	23	11	23	11
direction	E	NNE	NE	NE	ENE	NE	NE	NE	ENE	SW	W	NW	SW	E	E
speed	2.7	2.6	2.3	5.0	5.6	7.4	6.3	5.2	4.0	2.0	9.3	6.5	7.4	3.6	5.1

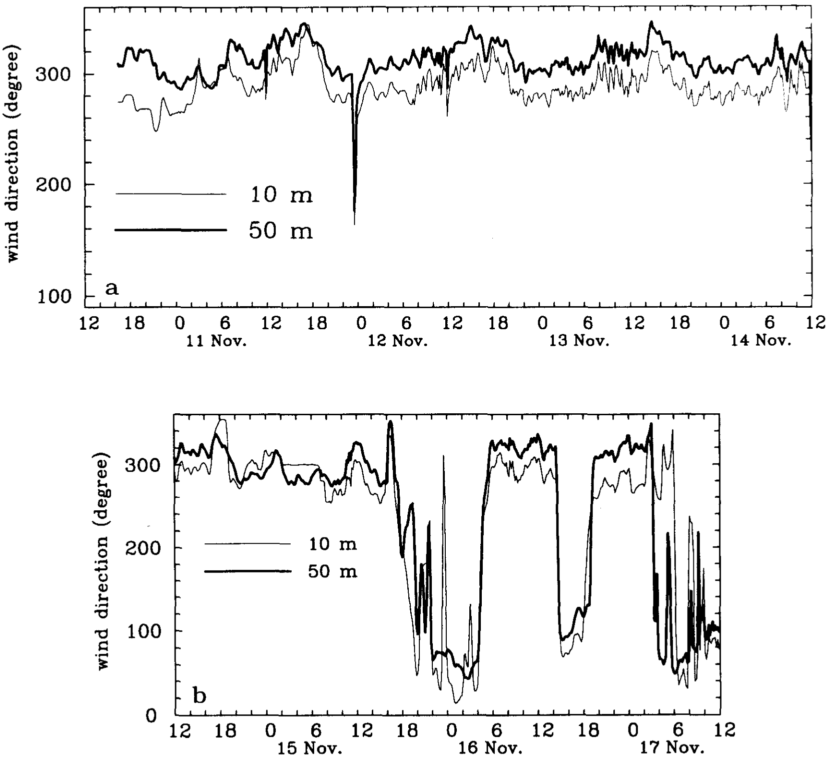

Fig. 3. Wind directions in 10 and 50 m for the period from 10–17 November 1989. The values are averages of 10 min.

u_g, v_g are the components of the geostrophic wind, f is the Coriolis parameter, p^* is the pressure deviation from hydrostatic, ρ_o is the air density, h the height of orography (see Fig. 4), and H the height of the terrain "outside" the valley. Note that u and v are both functions of the coordinate across the valley y and of the height z.

We evaluated these equations for our observed wind conditions ranging from NNE to ENE and determined the trajectories of the wind in the Prandtl layer (in approximately 15 m). The results are displayed in Fig. 4b for a geostrophic wind velocity of 5 ms^{-1}. In Fig. 4a, the cross section of the model valley is illustrated. We see that for all three cases the northeasterly winds outside the valley are deflected towards the east. This results in northwesterly winds in the valley as have been observed between 10–14 November (Fig. 3). Apart from the channelling, a counter current results for these cases for the innermost 100 km of the valley. In addition, for the case of NNE geostrophic wind the cannelled surface wind velocity in the center of the valley even exceeds the geostrophic wind speed by 2 ms^{-1}. This effect was, e.g., observed on 10 November, 23:00 when the wind speed in 850 hPa was 2.6 ms^{-1} coming from NNE (see Table 1) and the wind speed in 30 m was 5 ms^{-1} (Fig. 5a).

The trajectories also show, that the airmasses in the surface level had a much longer residence time in the valley than those in the upper levels above the valley. Consequently, the air at the measuring site had already travelled 240 km for the NNE case, 140 km for the NE case, and 80 km for the ENE case in the valley for 26, 23, and 19 h. respectively bringing air from the western, northwestern and northern part of the Po Valley to the observation point. In this area most of the Italian industry and large cites like Milan and Turin are located loading the air with pollutants.

This investigation gives a clue on the origin of air measured at San Pietro. However, we are aware

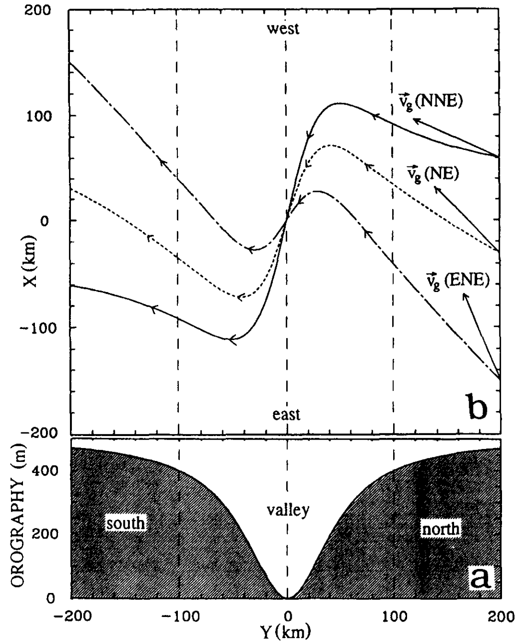

Fig. 4. (a) cross section through idealized model valley; (b) surface wind trajectories for 3 different directions of the geostrophic wind.

of the fact that the results have been derived assuming an idealized valley, which does not consider the steep flanks of the Alps and the Apennines. To remedy this deficiency, a complete numerical modelling of the complex Po Valley, Apennines and Alpine terrain would be necessary.

3.4. Satellite observations

In the current investigation the polar-orbiting platforms NOAA-10 and NOAA-11 with a ground resolution of $1.1 \times 1.1\ km^2$ at the nadir trace were also used. Following a sun-synchronous orbit each satellite covers the Po Valley region $2\times$ a day. NOAA-10 passes in the morning (between 6:00 and 8:00 UTC) and in the evening (between 17:00 and 19:00) whereas NOAA-11 reaches the Po Valley at night (1:00–3:00) and at noon (11:00–13:00). The scan of the whole track (approximately 5000 km in length and 2500 in width) is about 15 min depending on the field of view of the receiving station. As a result, the scan time for the entire Po Valley region is less than one minute. The AHVRR (Advanced Very High Resolution Radiometer) imager onboard of the

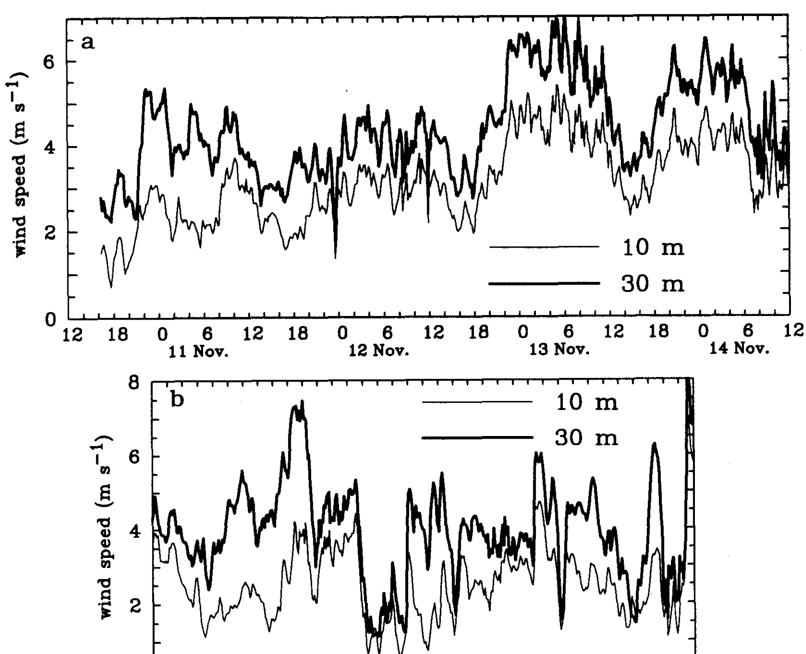

Fig. 5. Wind speed at 10 and 30 m for the period from 10–17 November 1989. The values are averages of 10 min.

NOAA satellite-series has 4 (NOAA-10) and 5 (NOAA-11) spectral bands, respectively. For the detection of fog, an image of temperature differences between brightness temperatures of channel 4 (10.5–11.3 μm) and channel 3 AHVRR (3.5–3.93 μm) ($T_4 - T_3$) can be used. Due to the low emissivity of fog in the spectral ranges of channel 3 compared with all other surfaces, a typical positive $T_4 - T_3$ value for the detection of fog has been found. Converting the channel 3 digital counts into brightness temperatures, the daytime signal includes not only the emitted radiance of the target but also an important part of reflected radiation related strongly to the spectral behaviour of the surface. Therefore, a shifting effect towards negative $T_4 - T_3$ values can be observed due to the high portion of reflected solar radiation of fog not observed for other surfaces. The binary fog masks presented in this volume (Fig. 6) were calculated from the $T_4 - T_3$ images using the threshold values suitable for the detection of fog published in Bendix and Bachmann (1991). Consequently, only fogs with a vertical thickness exceeding 20 m were registered.

Next to this fog classification algorithm, a method for geo-referencing the binary fog masks is necessary. Therefore an algorithm was developed (Bachmann and Bendix, 1992) which corrects image distortions due to the earth's curvature and the scanning procedure as well as the rectification to the Universal Transverse Mercator-grid-system of the Italian topographic maps. The accuracy finally gained with this algorithm for the figures presented in this volume is smaller than 1 km in longitudinal and latitudinal direction.

From the 20 NOAA satellite images evaluated

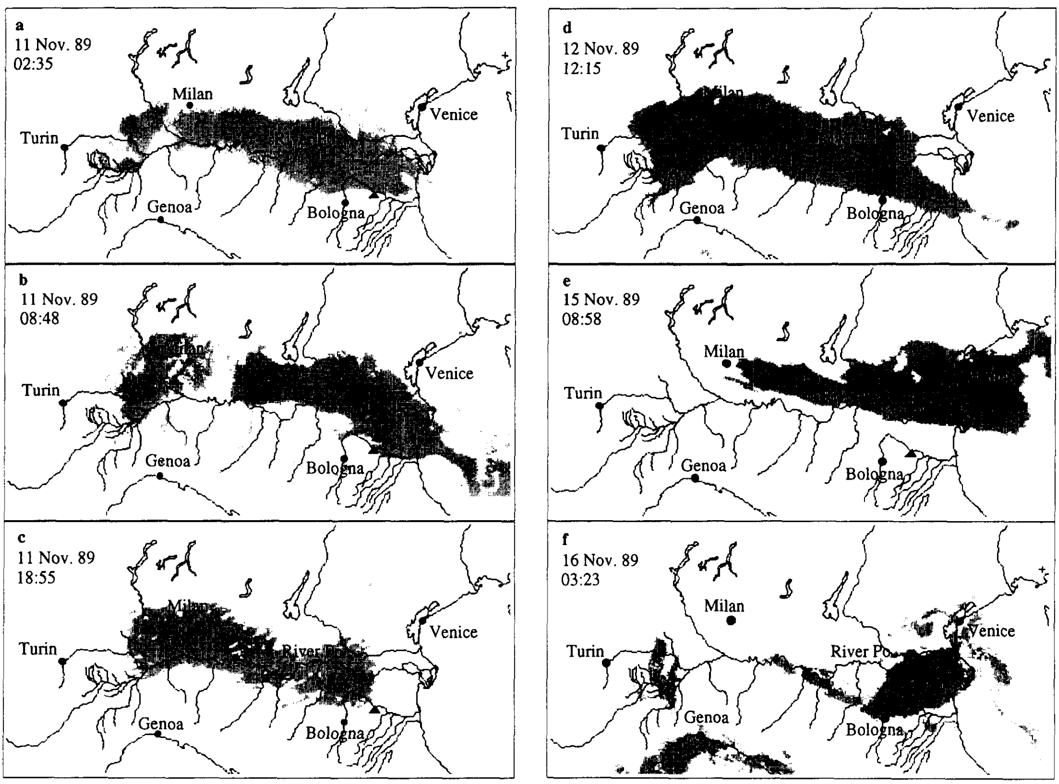

Fig. 6. Satellite pictures of NOAA-10 and 11; shaded areas represent areas covered with fog. (a = 11 November at 2:35, b = 11 November at 8:48, c = 11 November at 18:55, d = 12 November at 12:15, e = 15 November at 8:58, f = 16 November at 3:23 local time). The gaps in the fog field in Fig. 6a and b do not represent fog-free areas; they are caused by a band of cirrus clouds in the higher troposphere.

for the period from 10–16 November 1989, 6 typical pictures are displayed in this paper (Fig. 6) and two in the paper of Fuzzi et al. (1992).

4. Discussion of the individual fog events

4.1. Event 1: 10–11 November 1989

The conditions for the first fog event were set already on 9 November where rain showers supplied the soil with sufficient water so that the volumetric liquid water in the first 10 cm measured 0.19 $cm^3\,cm^{-3}$ at 17:30. As the clouds disappeared in the afternoon of 10 November ideal conditions for the development of radiation fog existed. The satellite picture of 10 November, 18:55 (not displayed here) already shows southeast of Milan a $70 \times 70\,km^2$ large field of patchy fog elements reaching higher than 20 m. However, no fog of this vertical extension was registered at the observational site.

Shortly before 17:00 the sunset was accompanied by a strong temperature decrease in all levels whereby the surface and the adjacent levels cooled fastest (Fig. 7). Consequently, supersaturation was reached early at 18:30 which was coupled to a first formation of shallow ground fog (Fig. 8). The fog stayed until 23:00 with LWC fluctuating between 50 and 100 $mg\,m^{-3}$. Only around 22:00, the shallow ground fog extended above 10 m and disappeared rapidly thereafter around 23:00. The only clue for this behaviour is given by the evolution of the surface winds.

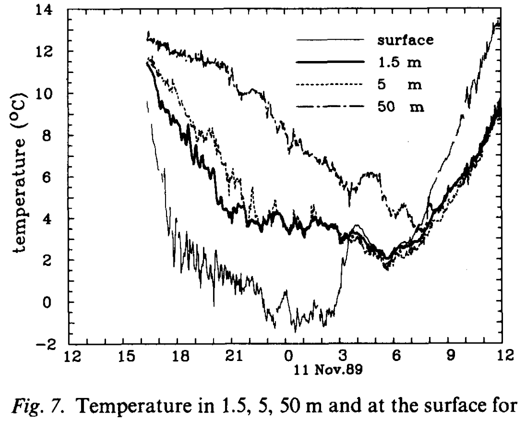

Fig. 7. Temperature in 1.5, 5, 50 m and at the surface for fog event 1, 10–11 November 1989. The values are averages of 2 min.

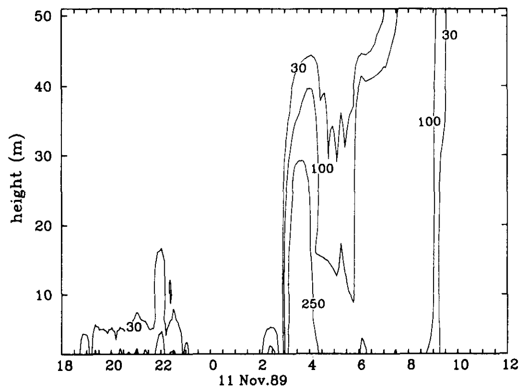

Fig. 8. Time evolution of the LWC as a function of height for fog event 1 on 10, 11 November 1989. LWC was obtained by a FSSP-100 at 1.5 m and a 2nd FSSP-100 moving with the tower elevator between 3 and 50 m altitude. The values used are 10-min averages in time and 5-m averages in height for the moving FSSP-100. The contour lines display the LWC in $mg\,m^{-3}$.

The sodar observations indicate in the afternoon a decrease in wind speed in the lower 150 m so that wind velocity in the early evening was minimal (Fig. 9). If we assume that "no sodar echo" is equivalent to "no turbulence", in the period from the fog onset at 19:00 until 22:00 no turbulent mixing occurred. The observation of the horizontal wind at the tower (Fig. 5a) displays that the wind increased again in 10 and later in 30 m when the fog formed and increased even more at 21:00. This can indicate a very shallow low level jet supporting the assumption of a turbulence free boundary layer. The changes in wind speed caused a vertical wind shear which was probably responsible for the beginning of a turbulent mixing in the surface layer below 50 m. This wind shear penetrated to 60 and 90 m between 22:00 and 0:00 (Fig. 9) and therefore most likely caused the short intensification and the later dissipation of the fog. A result of the turbulent mixing might also have been the weak increase in the water vapour mixing ratio (Fig. 10) after 21:00 as well as the enhanced temperature decrease in 50 m (Fig. 7).

Summing up the results, we note that this first shallow fog was caused by radiative cooling in a very stable surface layer and disappeared probably due to turbulent mixing processes.

From the satellite pictures (Fig. 6a) at 2:35, we can see that a huge fog field has formed covering

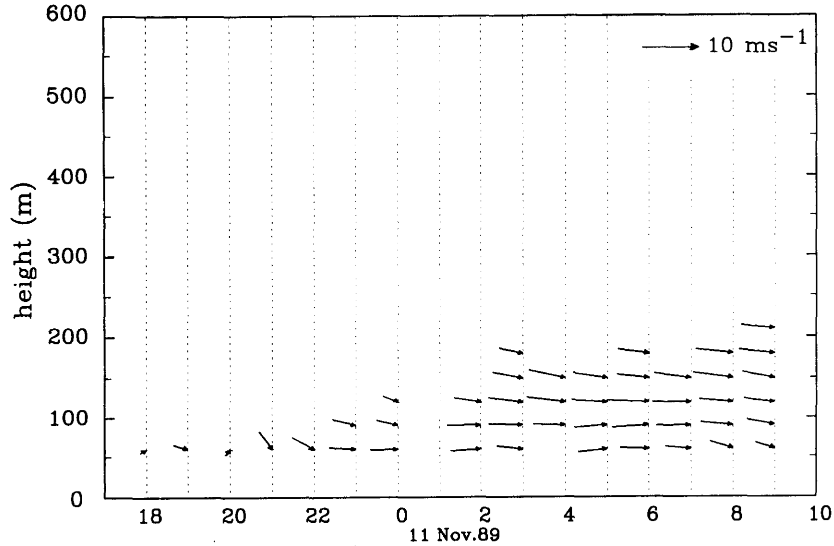

Fig. 9. Horizontal wind observed with the Doppler Sodar for fog event 1 on 10, 11 November 1989. (Data used are 1 h averages; the vector arrow in the upper right corner defines a west wind of 10 ms^{-1}.)

nearly the entire Po Valley. However, we can see that the observational site is just outside the southern edge of the fog field. There at 3:00 new fog appeared. Temperature and water vapour mixing ratio decreased in the 50 m level (Fig. 7, 10), causing a relative humidity close to saturation. The fog instantaneously reached up to 40 m (Fig. 8) and the surface temperature made a jump of 3 °C. As this jump is only weakly reflected in the curves for the air temperature, we can conclude that it was mainly caused by radiative heating due to the thermal radiation of the fog layer itself. The fog top dropped 20 m in the period from 4:30 to 5:30 which was connected to a temperature increase in 50 m and an increase in wind speed in 30 m (Fig. 5a).

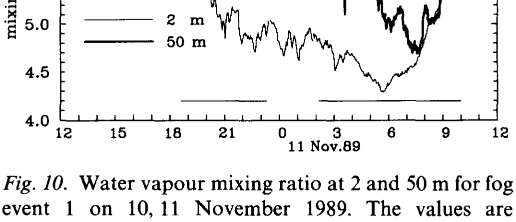

Fig. 10. Water vapour mixing ratio at 2 and 50 m for fog event 1 on 10, 11 November 1989. The values are averages of 2 min. The horizontal lines at the lower and upper border indicate the time periods with supersaturation in 2 and 50 m, respectively.

After 5:50, the fog height grew again to 40 m and exceeded the maximum observation height of 50 m at 7:00. The air temperature near the surface increased while the 50 m temperature decreased presumably due to the radiative cooling near the fog top until finally at 7:00 the first 50 m became isothermal.

From the gathered information, we cannot deduce clearly why the second fog episode took place. Two explanations for this type of fog appearance are possible: either the fog field developed elsewhere and was advected to the observation point or the vertical mixing became effective at 3:00 transporting water vapour into the surface layer. Supporting the explanation of advection is the fact that parallel to the onset of fog the concentration of nitrogen oxide (Kessel et al., 1992) and the number of unactivated aerosol particles increased significantly. (Both can be used as an indicator for horizontal transport processes.) The second hypothesis seems reasonable if one looks at the sodar data (Fig. 9) which confirm the existence of turbulent mixing especially during the fog intensifications. Nevertheless, the first hypothesis for the reason of fog appearance seems more reasonable since the LWC increases quite rapidly and the fog character is similar to other advected fog fields which were observed in the following events 2 and 4.

At 9:00, the fog disappeared rapidly. As the sun rose already at 7:00 temperature increased during this time in all levels (Fig. 7). The fog field disappeared over all heights nearly at the same time. Only a time lag of some few minutes between fog dissipation at the ground and the dissipation aloft could be detected by the FSSP observations (Fig. 8). Looking at the satellite pictures at 8:58 (Fig. 6b) it becomes obvious that we were again just at the edge of a seemingly eastward drifting fog field.

During daytime, the fog field thinned out so that satellite images at 14:06 (11 November) showed fog only for isolated areas in the Center of the Po Valley (Fuzzi et al., 1992).

4.2. Event 2: 11–14 November 1989

During the night of 10–11 November, the ground temperature inversion rose from 200 m at 23:00 to 450 m in the morning hours. This inversion persisted the entire following day since the solar radiation only generated a boundary layer of 250 m. In this well-mixed layer, the warm air was loaded with water vapour from the open water surfaces and the moist soil in the valley.

During the formation phase of this long-lasting fog, two different processes can be detected. At the beginning, the formation of fog shows clearly a radiative character. The temperature decreased in the afternoon of 11 November near the surface while the 50 m level experienced almost no cooling (Fig. 11). Furthermore, the curves for the concentrations of nitrogen oxide (Kessel et al., 1992) from 18:00 until 20:00 support this assumption, as the gradients are similar to those in other radiative nights with extremely high values of 25 (nmol m^{-3}) m^{-1}. Supersaturation at ground level was reached about 19:00 and fog persisted at this time only near the surface.

Shortly after 20:00, fog extended over the entire 50 m and the liquid water content reached over to 300 mg m^{-3} (Fig. 12). Correspondingly, the temperature jumped from 10 to 3°C in about 10 min in the 50-m level, wind speed (Fig. 5a) in the lower 10 m increased, wind direction (Fig. 3a) changed from 340 to 290°, and the water vapour mixing ratio dropped by 2 g kg^{-1} (Fig. 15 to follow). Thus, this sudden vertical expansion of the fog field at the measurement site was certainly caused by the advection of an already existing cold and high reaching fog layer. This is supported by the satellite image at 18:55 (Fig. 6c) which shows that a large fog field in the Po Valley had formed again.

The evolution of the liquid water content during the three following fog nights was quite similar. The fog reached its maximum LWC shortly after sunset (except for the 11th where the initialisation of the fog proceeded) and decreased afterwards slowly (Fig. 12). The maximum values of the liquid water content were in the first two days with 350 mg m^{-3} a little bit higher than on the third day where at most 250 mg m^{-3} were observed. During all 3 fog nights the entire Po Valley was

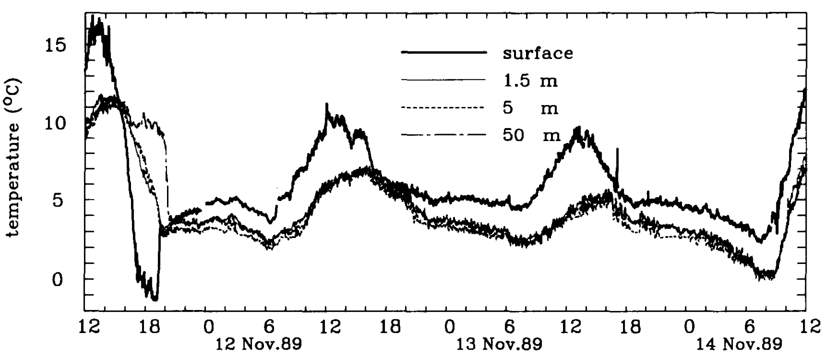

Fig. 11. Temperature in 1.5, 5, 50 m and at the surface for fog event 2, 11–14 November 1989. The values are averages of 2 min.

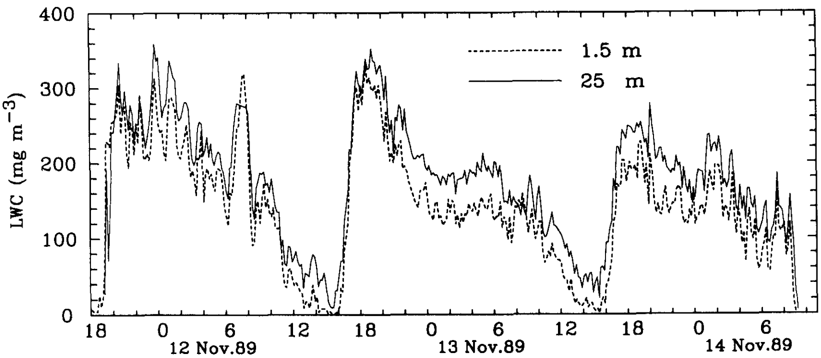

Fig. 12. Time evolution of the LWC in 1.5 and 25 m for fog event 2, 11–14 November 1989. The values are averages of 2 min.

covered with fog even extending several 10 km into the Adriatic sea (see Fuzzi et al., 1992).

During the daytime, the fog weakened significantly in the surface levels. Fig. 12 illustrates that LWCs as low as 20 mg m^{-3} were observed between 13:00 and 16:00 in the ground level. The LWC in the 25 m level remained higher with values between 40 and 80 mg m^{-3}. From the satellite figure on 12 November (Fig. 6d), we can see that the huge fog field shrunk during daytime especially at its north eastern rim. This was also valid for the day time period on 13 November (see Bendix and Bachmann, 1991).

The weakening of the fog near the ground was due to the heating of the surface by solar radiation of around 200 W m^{-2} which consequently resulted in upgoing heat fluxes and warming of the air (see temperature maxima in Fig. 11). Looking at the two curves for the short-wave radiation (Fig. 13), it is interesting to see that the 50-m level clearly experienced higher solar fluxes. Thus, Fig. 13 is also a representation of the divergence of the downwelling short-wave radiation fluxes.

The subsequent intensification of the fog at 17:00 on 13 and 14 November occurred, as far as the FSSP tower observations are concerned, in all levels at once. This enhancement is certainly effected by the net radiation flux which became negative in the late afternoon and consequently the temperature decrease caused an increase in relative humidity and supersaturation, respectively.

The intensifying fog was in all cases coupled to an increase of the horizontal wind speed (Fig. 5a) which reached, in 10 m, values up to 5 m s^{-1} and in 30 m up to 7 m s^{-1}. Furthermore, the sodar observations (Fig. 14) show that the wind above 60 m also increased during night time shortly before or at midnight which was true for the entire period (11–14 November). In the 1st and the 3rd nights, strong wind shears were observed while in the 2nd night (12/13 November), the winds were the same in all heights. Maybe this gives a hint why the LWC in the first and last nights (Fig. 12) displays quite strong fluctuations in contrast to the LWC in the second night (12/13 November), which experienced only smaller short-term variations. During daytime, however, the wind velocity in general decreased.

A comparison of the highest sodar echos with the incoming short-wave radiation flux near the ground shows that the fog height was mostly identical with the highest sodar echo observed. From this, we can conclude (Fig. 14) that the fog height was quite constant during the 1st day (12 November); during the 2nd day, however,

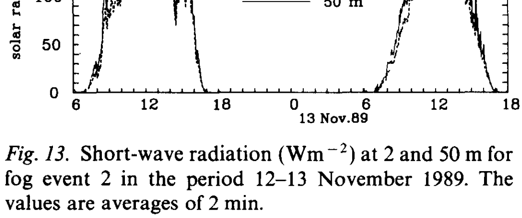

Fig. 13. Short-wave radiation (Wm^{-2}) at 2 and 50 m for fog event 2 in the period 12–13 November 1989. The values are averages of 2 min.

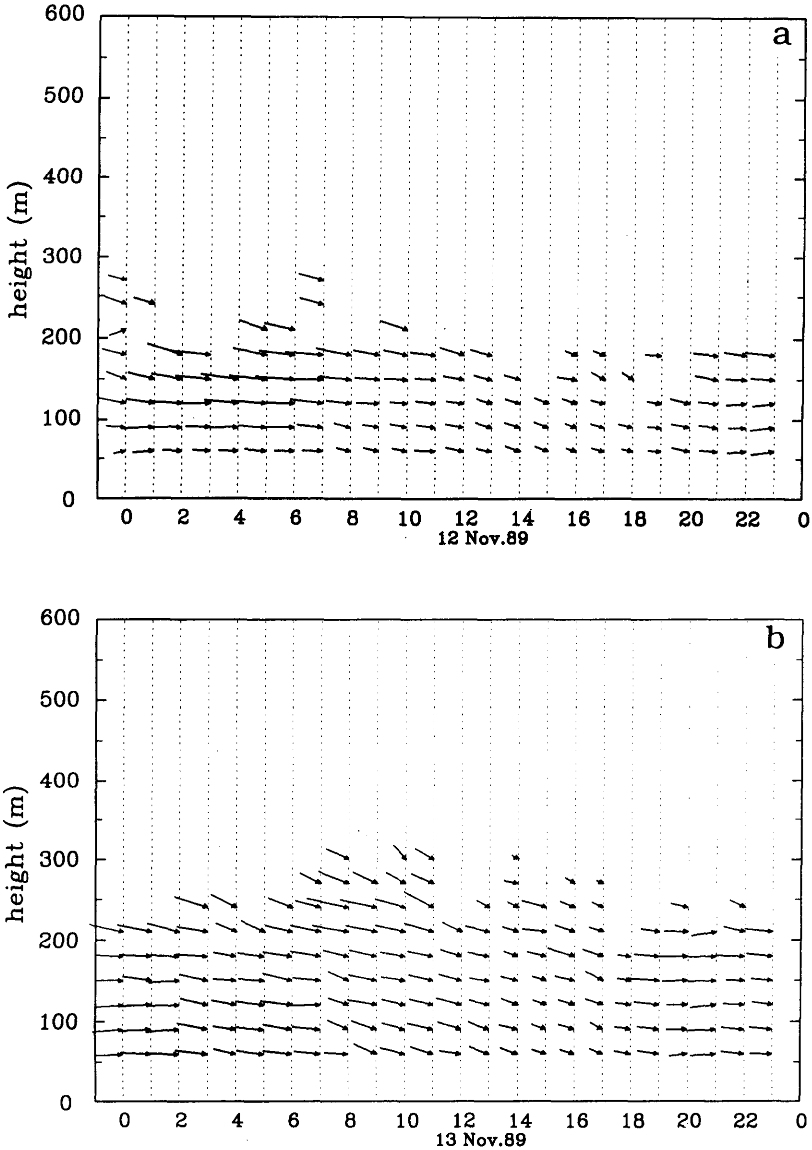

Fig. 14. Horizontal wind observed with the Doppler Sodar for fog event 2, 11–14 November 1989. (cf. Fig. 9).

strong irregularities on the fog top appeared. The top of the fog ranged around 150–180 m in the period from the evening of 11 November until the early morning of 13 November. Afterwards, the fog height seemed to fluctuate between 180 and 240 m. The temperature profile from the balloon sounding which are not displayed here confirm a fog height of 150 to 200 m.

The reason for the final dissipation of the fog on 14 November is hard to detect as nearly all variables were very similar in all three mornings. The FSSP observations on the tower (Fig. 12) do not clearly indicate if the fog dissipated faster near the surface than aloft due to the time lag caused by the motion of the tower elevator at 9:00. Nevertheless the relative humidity at ground

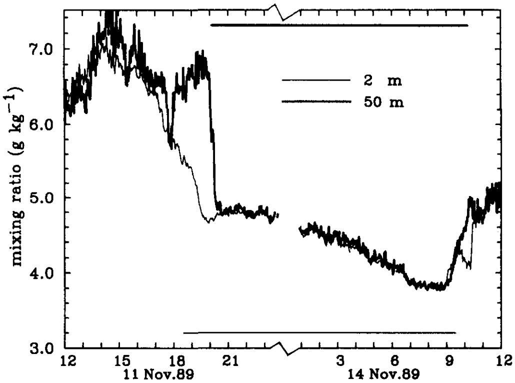

Fig. 15. Water vapour mixing ratio for the beginning and the end of fog event 2, 11 and 14 November 1989. The values are averages of 2 min.

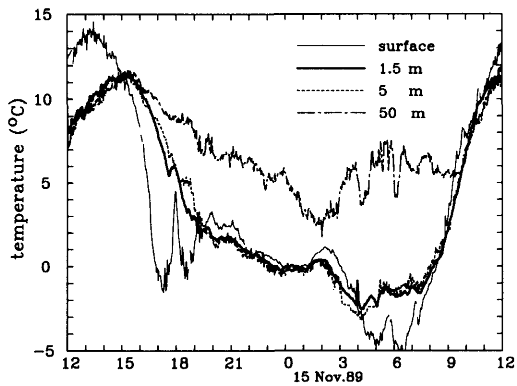

Fig. 17. Temperature at 1.5, 5, 50 m and at the surface for fog event 3, 14, 15 November 1989.

started to decrease earlier than in the 50-m level which is caused by the decreasing mixing ratio in 2 m at 10:00 (Fig. 15). Obviously, the observational site was at the southern edge of the fog field where warm and dry air was advected.

4.3. *Event 3: 14–15 November 1989*

As the ground temperature inversion up to 450 m still persisted and a large part of the Po Valley was fog free during day time, the lower 200 m could again take up a significant amount of water vapour.

In contrast to the previous fog events, the fog during this night had extremely high LWCs up to 500 mg m^{-3} (between 20:00 and 20:30 in ground level, no contour line was displayed) and strong vertical LWC gradients (Fig. 16). The fog formation phase near the surface between 18:00 and 19:00 was caused again by radiative cooling as can be seen from the temperature and humidity evolution (Fig. 17, 18). At 19:30, the very shallow ground fog suddenly expanded to above 50 m (Fig. 16). According to the balloon soundings at 20:00 the fog top reached up to 85 m.

As already described in fog event 1, the reason for the sudden vertical growth of the fog could either be the mixing in of humid air from above or the advection of an already existing fog field. If we assume that vertical turbulent mixing was dominant, one would expect that next to the humidity increase, the temperature near the surface would also increase and the temperature in 50 m should

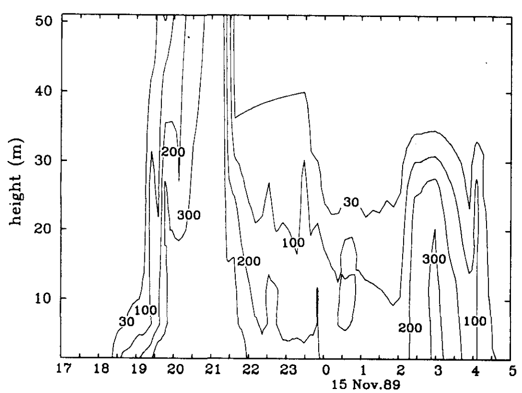

Fig. 16. Time evolution of the LWC as a function of height for fog event 3, 14, 15 November 1989.

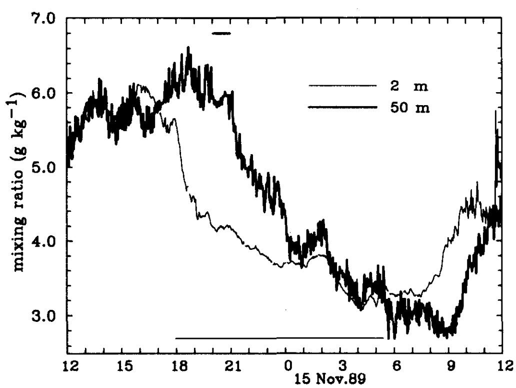

Fig. 18. Water vapour mixing ration at 2 and 50 m for fog event 3, 14, 15 November 1989.

decrease. Fig. 17, however, shows that both temperatures decrease simultaneously so that a temperature gradient of more than 5°C/50 m was maintained.

If we assume, on the other hand side, that a huge fog field as in event 2 was advected, it is surprising that the temperature and the LWC showed such strong gradients. In an aged and well-mixed fog field, no such gradients for temperature and LWC should occur (compare Figs. 11 and 12). Another effect contradicting the advection theory is the very slow growth of the LWC. In addition, the high LWC indicates that the fog generated close to the observation point since it would not have survived a large horizontal transport. Thus, neither two of the explanations for the sudden vertical expansion of the fog is satisfactory. Therefore, another interpretation of the measurements is suggested: analogously to the beginning of event 1, the onset of this fog was caused by radiative cooling, while the water vapor mixing ratio and temperature decreased in the ground level. In contrast to this, in 50 m, only the temperature decreased, while the water vapor mixing ratio, increased (Figs. 17, 18). Thus, the advection of cold and moist air was most likely responsible for the extreme fog intensification in both height and LWC.

At 21:00, the fog in the upper level (above 30 m) dissipated as rapidly as it was generated and the LWC near the surface decreased significantly. This sudden dissipation and reduction in LWC can be explained by a cut-off from the supply of water vapor by horizontal advection (Fig. 18). Consequently, relative humidity in 50 m dropped down to 75% and the remaining fog layer weakened.

Around 2:00, the fog intensified again in height and LWC due to the renewed horizontal advection of water vapour (Fig. 18). The fog top, however, only reached up to 30–35 m as the advection of water vapour in 50 m only sufficed for a relative humidity of 95%. After 2:00, we noticed a complete decoupled behaviour of the ground layer and the layers above 30 m. Aloft the wind speed increased after 2:00 while the wind in 10 m still decreased until 4:00 (Fig. 5). The temperature evolved similarly. For the 50 m level, we detected a strong advection of temperature with low water vapour concentrations (Fig. 18). Temperature in the surface layer, however, dropped to −2.5°C and experienced the advection of warm air only after 4:30 what was responsible for the dissipation of the fog. This unexpected early end of the fog was most likely caused by the subsiding dry air of the high pressure system which finally penetrated the ground inversion. The balloon sounding at 11:00 on 15 November showed an almost isothermal profile in the lower 500 m. From satellite images of 15 November, 8:58 (Fig. 6e), we can see that first the entire southern part of the Po Valley was fog free with a sharp southern edge of the fog field. The remaining fog field did not persist during daytime as reported by the satellite images at noon time and in the evening which detected a completely fog free Po Valley on 15 November.

4.4. *Event 4: 15–16 November 1989*

In contrast to the previous fog nights the fog formed significantly later, i.e., at 22:45 (Fig. 19). Comparing the relative humidity from 14 November with 15 November at 17:00, we found that on the 14th, the relative humidity was higher than 80% while on the 15th the relative humidity was around 55%. Until the onset of the fog, temperature (Fig. 20) and mixing ratio (Fig. 21) showed very strong fluctuations in all levels. These oscillations are often observed in the nocturnal stable surface layer prior to fog formation (Jiusto and Lala, 1983; Fitzjarrald and Lala, 1989).

Fog suddenly formed at 22:45 with an observed height of about 30 m (Fig. 19). As the temperature near the surface didn't change remarkably, but the water vapor mixing ratio increased strongly (Fig. 21), it is evident that the spontaneous fog formation was caused by moist air advection.

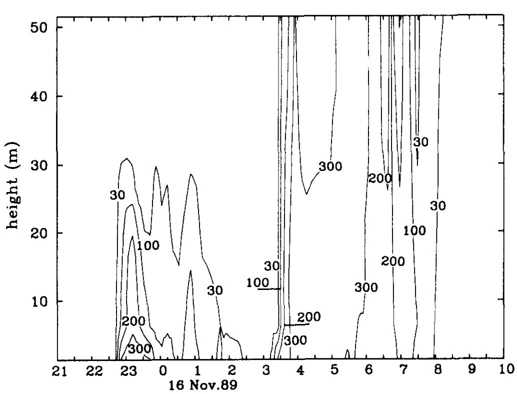

Fig. 19. Time evolution of the LWC as a function of height for fog event 4, 15, 16 November 1989.

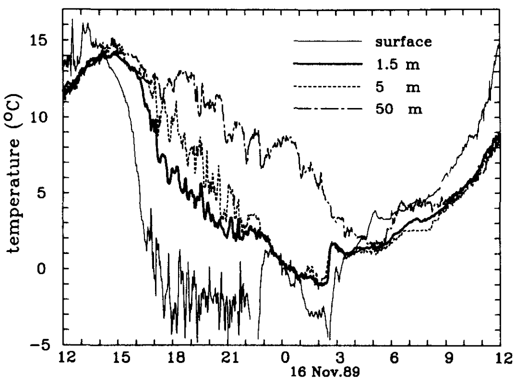

Fig. 20. Temperature at 1.5, 5, 50 m and at the surface for fog event 4, 15, 16 November 1989.

The supply of water vapour during this moist air advection lasted only for a short time so that already after 30 min, the fog weakening and dissipation started. The weakening is accompanied from 23:00 by a significant decrease in temperature and mixing ratio; consequently, dense fog only remained till 1:00 in the lowest few meters. Finally, at 1:00, cold air also became dominant at the 50 m level which cooled rapidly from 9° to 4°C in 2 h and caused a fast increase in relative humidity.

At 2:30, the relative humidity at 50 m was already at 100%, air at 2 m, however, was for a short time subsaturated. As no measurements of the tower FSSP are available at 3:00 at 50 m, we cannot confirm that the fog already extended all the way to this altitude as indicated by the relative humidity. The surface temperature confirmed the existence of an elevated fog layer as it experienced a jump from −5° to 0°C shortly after 2:30. The extreme jump in the air temperature, however, observed at the same time can only be explained by the advection of warm air.

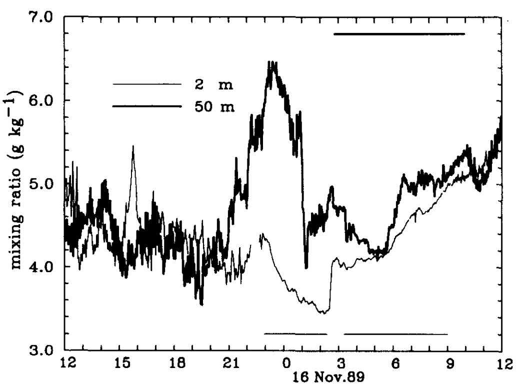

Fig. 21. Water vapour mixing ratio at 2 and 50 m for fog event 4, 15, 16 November 1989.

At 3:15, the air next to the surface finally became again supersaturated in agreement with the observed LWC and fog was reported over the entire observation height. Due to the strong and fast increase in LWC, we can assume that an already existing fog field was advected. From 3:15 until 4:30, weak gradients of temperature and LWC were still observed between the surface and 50 m. After 4:30, these gradients disappeared and the fog displayed a well-mixed character as previously encountered in event 2 (Figs. 11–13). The assumption of a moving fog field is supported by the satellite image of 16 November at 3:23 (Fig. 6f) which shows that the observational site is just covered by the southern rim of the fog field. The horizontal extension of this fog field is much smaller than in the previous nights. This difference resulted from the fact that during daytime of 15 November, the ground inversion was destroyed and dry air from above was mixed into the boundary layer. The newly developing ground inversion extended only up to 100 m at 23:00 and to 200 m in the morning.

The weakening of the fog started at 6:00 when advection of warmer air over all levels occurred. The deterioration of the fog was enhanced at 7:00 by the sunrise and the associated warming of the surface. The fog dissipated shortly after 8:00 near the ground and around 8:30 in the level above 25 m. This was the only time that we clearly observed a disappearance of the fog that started near the surface.

The winds during that night changed from the typical northwest winds to rotating weak winds after 16:00 until 21:45. Then the wind increased again having east-northeast directions until 4:00 when the old conditions of northwesterly winds were reestablished. Furthermore, in the morning of 16 November, a cold front formed along the Adriatic Sea starting in the upper atmospheric levels. Its influence certainly also has to be considered, as during the entire day (16 November), the sky was partly covered with clouds and elevated fog fields, respectively. This cloud cover disappeared in the late afternoon.

4.5. *Event 5: 16–17 November 1989*

Comparing this event with the 4 previous ones this is the shortest fog episode with the lowest fog top. At the 25 m and 50 m levels, the tower FSSP never reported any LWC, in agreement with the observations of humidity at 50 m which always showed subsaturation (Figs. 22 and 24). The few observation points between the ground and the 25 m level due to the moving of the tower FSSP indicate that the LWC reached up to 150 mg m^{-3} between 10 and 20 m for a short time interval. Only 3 ascents were done during the fog episode; thus, the data for Fig. 22 are interpolated between the observation points at 1:00, 2:00, and 3:00.

On the evening of 16 November, strong radiative cooling occurred, which decelerated at 19:00 and lead to temperature fluctuations similar to those of the previous fog night (Figs. 20 and 21). The strong drop of temperature from 18:00 to 19:00 (Fig. 23) as well as the simultaneous jump in mixing ratio (Fig. 24) was presumably supported by horizontal advection processes. The cooling ended by a sudden increase in surface temperature of 3°C at 19:00. This heating of the surface is a result of thermal radiation from above, i.e., a cloud or a patch of low stratus crossed the observational site. This passing cloud lasted for only 1 h, so that at 20:00, the cooling of the surface and the adjacent air continued at about 0.5°C h^{-1}.

At 0:30 when fog formed, the temperature near the surface dropped again significantly to values below 0°C. The water vapor mixing ratio evolved analogously. Thus, one explanation for the formation of this fog is the advection of cold air. On the other hand, the advection of a single parcel of ground fog can neither be ruled out. In agreement with the slow increase in LWC during this period, however, it seems more probable that fog formation and development took place immediately at the observational site or in its close vicinity. Shortly after 2:00, the advection of cold air changed to the advection of warmer air and consequently the fog dissipated. As the air temperature at the end of the night still increased, no further fog formation was observed.

The increase of the surface temperature at 3:00 and 6:00 further indicates (Fig. 23) that clouds in higher altitudes crossed over the measuring site. This was confirmed in the morning by a cloud covered sky.

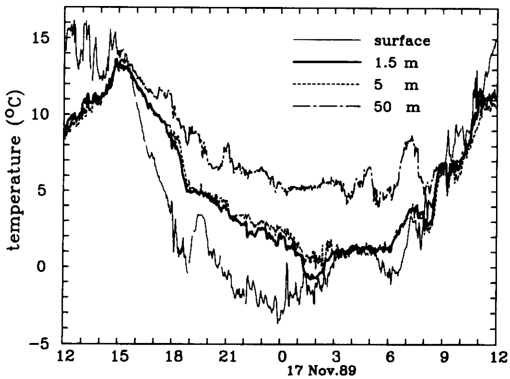

Fig. 23. Temperature at 1.5, 5, 50 m and at the surface for fog event 5, 16, 17 November 1989.

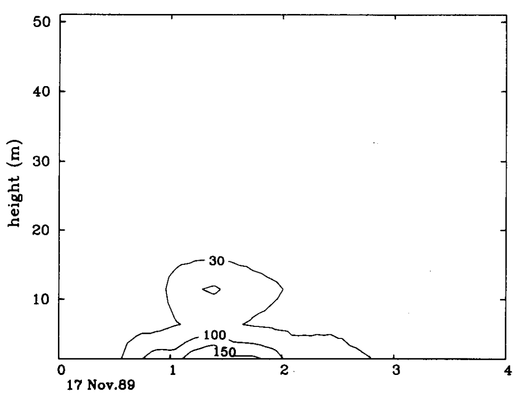

Fig. 22. Time evolution of the LWC as a function of height for fog event 5, 16, 17 November 1989.

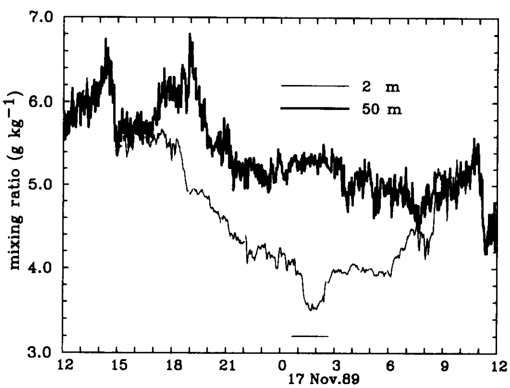

Fig. 24. Water vapour mixing ratio at 2 and 50 m for fog event 5, 16, 17 November 1989.

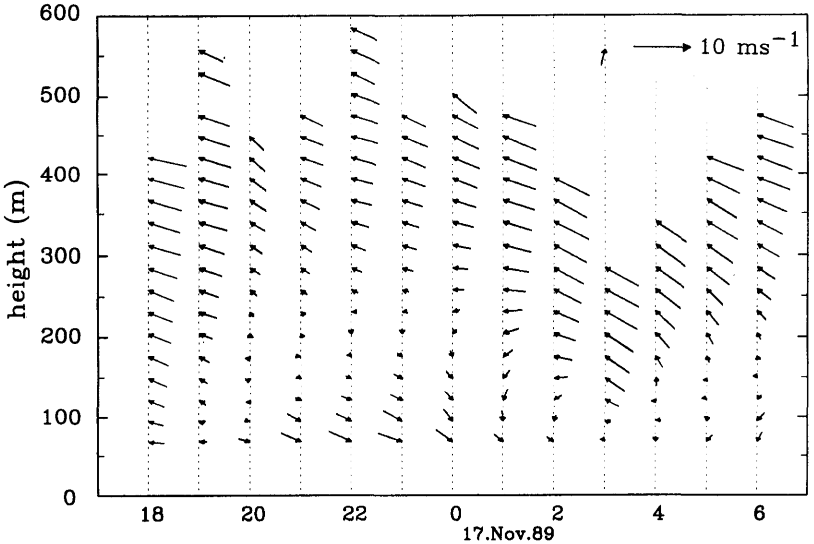

Fig. 25. Horizontal wind observed with the Doppler Sodar for event 5, 16, 17 November 1989. (cf. Fig. 9).

As the temperature at 50 m evolved again quite decoupled from that next to the surface, we can conclude that also in this night, the boundary layer was stably stratified. According to the sodar observation, however, the turbulent conditions of the layers were sufficient to reflect an echo. Thus, wind measurements up to 600 m are available, which show that the wind at the height above 300 m came during the entire night from east and east-southeastly directions (Fig. 25). In the first 100 to 150 m, however, the wind direction was west-northwest during the first half of the fog night. Furthermore, the wind speed even increased with decreasing height below 200 m and reached its maximum between 30 and 60 m (cf. Fig. 5b). This wind profile in the lower 200 m represents dramatically the channelling and counter-current wind phenomenon in the Po Valley. At the same time (around 1:00), when fog formed near the surface, the sodar echo indicates that the wind direction started to turn and the wind speed decreased. The surface wind rotated from north-west over north to northeast. This was caused by the branch of a cold front belonging to a cyclonic system with its center over the Black Sea which drifted westwards and influenced the observation site (Fig. 1e). Consequently, deep cloud cover was present in the morning which lasted until noon.

5. Summary and conclusions

From 10–17 November 1989 a joint fog field campaign was performed in the Po Valley in Italy by various research groups working together in the EUROTRAC subproject GCE (= ground based cloud experiment). During this period, a huge, blocking anticyclone developed and persisted over Central Europe and due to the cloud free atmosphere the radiative cooling in the nights caused a temperature inversion favoring fog formation especially in moist valleys as, e.g., the Po river valley. This is illustrated by the weather charts of the surface and 500 hPa level as well as by satellite pictures. Back-trajectories for the large-scale flow were calculated, illustrating the origin of air masses reaching the observation site. It was found that the airmasses changed significantly during the fog event 2 (11–14 November 1989) which was reflected by a drastic change in the pollution of the fog water (see Facchini et al., 1992).

At our measuring site in San Pietro Capofiume, the observed surface winds came from directions almost opposite to the large scale flow. This was a result of the channelling of the valley, even producing a counter current. This phenomenon was verified by means of an analytical model which also showed that surface air experienced a long transport along the valley and therefore contributed substantially to the strong pollutant concentration found in the fog water.

During the field campaign, 5 fog events were observed whose micrometeorological evolutions were discussed. Hereby 4 different types of fogs and/or fog formations can be suggested at the measuring site.

The first one was a pure radiation fog which was encountered only on the first half of event 1. The second type was a well-mixed and high-reaching fog layer which was developed elsewhere and was advected to the observational site. This type of fog was observed during the entire event 2, during the 2nd part of event 1 as well as the 2nd period of event 4. The 3rd and 4th types formed at the observation site due to advection of moisture and cold air, respectively. Moisture advection was most likely responsible for fog formation on event 3 and on the first period of event 4, while cold air advection influenced mainly event 5.

Furthermore, the observational results show that there is a clear difference between the height of the advected fog field and the height of the 3 other types of fogs. The advected fogs reached up to 80–200 m; the others were lower than 30 m. This significant difference was also found by Fitzjarrald and Lala (1989) for the Hudson river valley fog. Consequently, they distinguished between boundary layer and surface layer fogs. Surface layer fogs form in very stable conditions when the surface layer is decoupled from the boundary layer below heights of 20 m and precede often boundary layer fogs. These extend up to 150 m and their formation is mainly determined by the dynamics of the nocturnal boundary layer. Fitzjarrald and Lala (1989) found, e.g., that the channelling of the wind in the valley has an important influence on the boundary layer fog. These findings were in principle confirmed by our investigations.

Surprisingly, the pure radiation fog was not the dominant species observed. The radiation effect, however, was present evidently during all events. During cloud and fog-free day time periods, the heating of the surface by the short-wave radiation was causing a moisture loading of the boundary layer. In the afternoon and in the early evening, the negative long-wave radiation budget conditioned the fog formation by cooling of the air with 3–4°C/h, thus increasing the relative humidity. Especially prior to and during the first fog night, the radiative cooling was also responsible for the development of the ground inversion. As event 1 has shown, however, the radiative cooling of the surface and the adjacent layers could only result in a very shallow and non persistent ground fog. For the formation of a high-reaching and persistent fog, additional processes as, e.g., mixing and advection were required. However, it cannot be ruled out that the radiation effect was more important in other areas of the Po Valley, supporting the formation of high-reaching, well-mixed and dense fog layers which were advected. We can speculate that those fog fields developed in moister areas closer to the river Po, which is supported to some extent by the satellite pictures (see Fuzzi et al., 1992).

From our observations, no statement on the rôle of turbulence for fog formation can be drawn. In the literature, fog formation is sometimes attributed to lulls in wind speed (Roach et al., 1976). We have observed, however, that fog formation was accompanied by wind increases as well as decreases.

Concerning the dissipation and disappearance of the fog fields, we could identify, beside the simple movement of the fog, 2 different mechanisms. One was the solar radiation in the morning and the subsequent heating of the surface and the adjacent layers, the other the advection of warmer and drier air at the edges of the fog field. Even for the case when fog persisted during day time, this effect could at least be recognized at the fog edges. The other mechanism was the penetration of the ground temperature inversion by the subsiding dry air from the high pressure system.

In order to gain further insights into the processes governing fog formation and dissipation three-dimensional mesoscale numerical simulations are required. Special emphasis should be put on the dynamics influenced by the complex orographic terrain of the Po Valley and its surroundings.

6. Acknowledgments

The invaluable contribution of A. Correggiari, S. Miserocchi, D. Correggiari, C. Foschini and I. Tarozzi during the field work is gratefully acknowledged. G. Bocchiolo, D. Galofaro, G. De Rocco and C. Giarota performed sodar and radiosonde measurements. Funds for this experiment were provided by: Bundesministerium für Forschung und Technologie, Projects 07EU276 and 07EU773, CNR-Progetto Strategico Deposizioni Atmospheriche Acide, Commission of the European Communities, Project EV4V-0084-C, and Ministry of Economic Affairs of the Netherlands. The Regional Meteorological service SMR-ERSA is acknowledged for allowing access to its meteorological data bank. We also want to thank L. Schütz and D. Hackenthal for giving us access to their trajectory model of the Mainz University. The station of S. Pietro Capofiume is managed by Assessorato Agricoltura, Regione Emilia Romagna. The Po Valley Fog Experiment 1989 was carried out within the project EUROTRAC, subproject GCE (Ground-based Cloud Experiment).

REFERENCES

Bachmann, M. and Bendix, J. 1992. An improved algorithm for NOAA-AHVRR image referencing. *Int. J. of Remote Sensing*, *13*, no. 16, Nov. 1992.

Bendix, J. and Bachmann, M. 1991. Ein operationelles einsetzbares Verfahren zur Nebelerkennung auf der Basis von AHVRR-Daten der NOAA-Satelliten. *Meteor. Rundsch. 43*, 169–178.

Choularton, T. W., Fullarton, G., Latham, J., Mill, C. S., Smith, M. H. and Stromberg, I. M. 1981. A field study of radiation fog in Meppen, Germany, *Quart. J. R. Met. Soc. 107*, 381–394.

Fitzjarrald, D. R. and Lala, G. G. 1989. Hudson Valley Fog Environments. *J. Appl. Meteor. 28*, 1303–1328.

Fuzzi, S., Facchini, M. C., Orsi, G., Lind, J. A., Wobrock, W., Kessel, M., Maser, R., Jaeschke, W., Enderle, K. H., Arends, B. G., Berner, A., Solly, I., Kruisz, C., Reischl, G., Pahl, S., Kaminski, U., Winkler, P., Ogren, J. A., Noone, K. J., Hallberg, A., Fierlinger-Oberlinninger, H., Puxbaum, H., Marzorati, A., Hansson, H.-C., Wiedensohler, A., Svenningsson, I. B., Martinsson, B. G., Schell, D. and Georgii, H. W. 1992. The Po Valley fog experiment 1989. An overview. *Tellus 44B*, 448–468.

Facchini, M. C., Fuzzi, S., Kessel, M., Wobrock, W., Jaeschke, W., Arends, B. G., Möls, J. J., Berner, A., Solly, I., Kruisz, C., Reischl, G., Pahl, S., Hallberg, A., Ogren, J. A., Fierlinger-Oberlinninger, H., Marzorati, A. and Schell, D. 1992. The chemistry of sulfur and nitrogen species in a fog system. A multiphase approach. *Tellus 44B*, 505–521.

Gerber, H., 1987. Forward-scatter meter for estimating 10.6 μm aerosol extinction. *App. Optics 26*, 539–544.

Jiusto, J. E. and Lala, G. G. 1983. *Radiation fog field programs, recent studies.* ASRC-SUNY, Publ. No. 869.

Kessel, M., Grieser, J., Wobrock, W., Jaeschke, W., Fuzzi, S., Facchini, M. C. and Orsi, G. 1992. Nitrogen oxides concentrations and soil emission fluxes in the Po Valley. *Tellus 44B*, 522–532.

Petterssen, S. 1956. *Weather analysis and forecasting.* McGraw-Hill Book Company, New York, Toronto, London, 428 pp.

Pilié, R. J., Mack, E. J., Kocmond, W. C., Rogers, C. W. and Eadie, W. J. 1975. The Life cycle of valley fog. Part I: Micrometeorological characteristics. *J. App. Meteor. 14*, 347–363.

Roach, W. T., Brown, R., Caughey, S. J., Garland, J. A. and Readings, C. J. 1976. The physics of radiation fog: I, a field study. *Quart. J. R. Met. Soc. 102*, 313–333.

Wattle, B. J., Mack, E. J., Pilié, R. J. and Hanley, J. T. 1984. *The rôle of vegetation in low-level water budget in fog.* ARVIN/CALSPAN Advanced Technology Center, No. DAAG29-82-C-0022, 33 pp.

Wippermann, F. 1984. Air flow over and in broad valleys: Channelling and Counter-current. *Contrib. Phys. Atmos. 57*, 92–105.